Enzalutamide, an Androgen Receptor Signaling Inhibitor, Induces Tumor Regression in a Mouse Model of Castration-Resistant Prostate Cancer

Javier Guerrero,[1] Iván E. Alfaro,[1] Francisco Gómez,[1]
Andrew A. Protter,[2] and Sebastián Bernales[1,2]*

[1]Fundación Ciencia & Vida, Santiago, Chile
[2]Medivation, Inc., San Francisco, California

BACKGROUND. Enzalutamide (formerly MDV3100 and available commercially as Xtandi®), a novel androgen receptor (AR) signaling inhibitor, blocks the growth of castration-resistant prostate cancer (CRPC) in cellular model systems and was shown in a clinical study to increase survival in patients with metastatic CRPC. Enzalutamide inhibits multiple steps of AR signaling: binding of androgens to AR, AR nuclear translocation, and association of AR with DNA. Here, we investigate the effects of enzalutamide on AR signaling, AR-dependent gene expression and cell apoptosis.

METHODS. The expression of AR target gene prostate-specific antigen (PSA) was measured in LnCaP and C4-2 cells. AR nuclear translocation was assessed in HEK-293 cells stably transfected with AR-yellow fluorescent protein. The in vivo effects of enzalutamide were determined in a mouse xenograft model of CRPC. Differential gene expression in LNCaP cells was measured using Affymetrix human genome microarray technology.

RESULTS. We found that unlike bicalutamide, enzalutamide lacked AR agonistic activity at effective doses and did not induce PSA expression or AR nuclear translocation. Additionally, it is more effective than bicalutamide at inhibiting agonist-induced AR nuclear translocation. Enzalutamide induced the regression of tumor volume in a CRPC xenograft model and apoptosis in AR-over-expressing prostate cancer cells. Finally, gene expression profiling in LNCaP cells indicated that enzalutamide opposes agonist-induced changes in genes involved in processes such as cell adhesion, angiogenesis, and apoptosis.

CONCLUSIONS. These results indicate that enzalutamide efficiently inhibits AR signaling, and we suggest that its lack of AR agonist activity may be important for these effects. *Prostate* © 2013 Wiley Periodicals, Inc.

KEY WORDS: androgen receptor; MDV3100; nuclear translocation; prostate cancer; microarray

INTRODUCTION

Prostate cancer is one of the most commonly diagnosed cancers in developed countries [1]. Growth and survival of early prostate tumors is highly dependent on levels of circulating androgens. Treatments such as androgen deprivation therapy (ADT), which typically includes suppression of testicular androgen by surgical castration or treatment with analogues of luteinizing hormone releasing hormone, are effective at slowing disease progression. In advanced disease, however, the cancer progresses despite low levels of circulating androgens that result from ADT. It had not

been appreciated until recently that despite the advancement of disease to castration-resistant prostate cancer (CRPC), the cancer cells remain dependent on androgen receptor (AR) signaling for growth [2]. The AR is a nuclear hormone receptor that is activated in response to the binding of androgens (e.g., testosterone and dihydrotestosterone [DHT]) in the cytoplasm to form the AR-ligand complex. The activated AR-ligand complex translocates to the nucleus where it dimerizes, binds co-activators and binds to DNA. The DNA-bound complex stimulates the transcription of genes that encode for proteins that regulate cell proliferation and survival [3]. The AR signaling pathway regulates the development and maintenance of normal prostate tissue and its deregulation is primarily responsible for the development, growth, and progression of prostate tumors [4]. Numerous efforts to understand the biology of CRPC have been undertaken [2,5,6] and several theories exist as to why prostate cancer progresses despite low to nonexistent circulating androgen levels. AR over-expression by either gene amplification, enhanced transcription, translation or alternative splicing as well as mutations in the AR ligand-binding domain (LBD), have been shown to contribute to the progression of prostate cancer to CRPC [7–11]. Increased AR expression, mutations or deletions in the AR LBD due to alternative splicing, are thought to result in constitutive activation of AR either in a ligand-independent manner or in the sensitization of AR to low levels of androgen present despite combined ADT [12]. The mutations in the AR LBD also result in the activation by most adrenal androgens, estrogens, progestins and even anti-androgens [13,14]. Although the mechanism remains unclear, sensitization of the AR to the low levels of androgen after ADT can result in agonist responses from antiandrogens such as bicalutamide [15–17]. Taken together, these data suggest that the AR signaling pathway continues to be important in CRPC and the development of therapies that efficiently and durably target this pathway are needed. Several human cell lines have been used to model prostate cancer (PCa) in cell culture. One such cell line, LNCaP, was derived from a supraclavicular lymph node metastasis of a human PCa. These cells depend on androgens to grow and respond to physiological levels of androgens-responsive genes such as the prostate-specific antigen (PSA) [18]. LNCaP cells carry a T877A mutation in the AR LBD that is frequently found in CRCP [19,20]. This mutation promotes cancer cell growth and survival by conferring tumor resistance to apoptosis [21] and allows AR to be activated by several steroids such as estrogens and the anti-androgens cyproterone and nilutamide [22]. In contrast, androgen independent C4-2 cells were isolated from castrated mice after sequential xenografts of LNCaP derived tumor cells (C4 cells) and are resistant to bicalutamide [9,23].

The novel rationally designed AR signaling inhibitor (ARSI) enzalutamide (formerly MDV3100) is a phenylthiohydantoin derivative with a sulfonamide side chain [24]. In a CRPC cell model system, enzalutamide has not only been shown to potently inhibit the binding of androgens to the AR, but also inhibit nuclear translocation and subsequent binding of the AR-ligand complex to DNA, thereby inhibiting transcription of AR target genes [25]. In contrast to antiandrogens (e.g., bicalutamide), enzalutamide does not induce agonistic effects on AR signaling in cells over-expressing wild type AR [25]. In a phase 3 placebo-controlled trial (AFFIRM, NCT00974311), enzalutamide was well tolerated and was shown to significantly increase overall survival by 4.8 months in patients with prostate cancer following docetaxel-based chemotherapy [26]. Enzalutamide was recently approved to treat late stage prostate cancer by the Food and Drug Administration and is commercially available as Xtandi. In this report, evidence is presented that distinguishes enzalutamide from antiandrogens and provides in vitro and in vivo xenograft evidence to support its effectiveness as a treatment for prostate cancer.

MATERIALS AND METHODS

Materials

Fetal bovine serum (FBS) was purchased from Gibco (Grand Island, NY). RPMI 1640 and DMEM/F12 culture media were obtained from Invitrogen (Carlsbad, CA). Hormone depleted (charcoal-stripped) dextran-treated FBS (CSS) was obtained from Gibco. Hygromycin-B and antibiotics were purchased from Gibco. Bicalutamide and DHT were purchased from Sigma (St Louis, MO). Enzalutamide was obtained from Medivation, Inc. (San Francisco, CA). Antibodies used for immunoblot assays were β-actin (#A5441) from Sigma and Caspase-3 (8G10, #9665) and Caspase-3 cleaved (Asp175, #9661) from Cell Signaling Technology (Danvers, MA). Ki67 antibody (NCL-L Ki67) from Novocastra (Leica Biosystems Newcastle Ltd., Newcastle, UK) was used in immunohistochemistry studies.

Cell Culture

LNCaP and C4-2 cells were purchased from ATCC (Manassas, VA) and cultured in RPMI 1640 culture media containing 10% FBS and 1% penicillin–streptomycin. For in vitro experiments, cells were androgen-

starved by growth in media containing 10% CSS and challenged with various concentrations of enzalutamide or bicalutamide.

Real-Time Quantitative Polymerase Chain Reaction (qPCR)

Total RNA was extracted using E.Z.N.A RNA extraction kit from OMEGAbiotek (Norcross, GA). cDNA synthesis was performed according to the manufacturer's protocol using 1 μg of RNA per sample and M-Mulv reverse transcriptase enzyme (Promega Corporation, Madison, WI). Quantitative gene expression analysis by real-time PCR was done using the Mx3005p qPCR system (Stratagene, Amsterdam, the Netherlands), TAQMAN probes and master mix (Applied Biosystem, Foster City, CA). TAQMAN primer sets: PSA: forward TGCCCACTGCATCAG-GAA, reverse GCTGACCTGAAATACCTGGCC, FAM-probe AAAGCGTGATCTTGCTGGGTCGGC, human TMPRSS2 (Hs00237175_m1) and human α 4[a] tubulin (Hs00428633_m1) were used. Quantitative PCR for each sample was done in triplicate; each reaction contained 2 μl of cDNA in a total volume of 20 μl. Calculation of the relative expression of the PSA gene was done by the comparative CT method [27]. The housekeeping gene α-tubulin was used for normalization.

Protein Extraction and Western Blotting

Cells were lysed with lysis buffer (50 mM HEPES, pH 7.4, 150 mM NaCl, 2 mM MgCl$_2$, 2 mM ethylene glycol tetraacetic acid, 1% Triton X-100, 10% glycerol, 2 mM phenylmethylsulfonyl fluoride, 2 μg/ml pepstatin, 2 μg/ml leupeptin, and 1 mM sodium orthovanadate) at 4°C. Equal amounts of protein from different treatments were resolved by SDS–PAGE and analyzed by immunoblotting with anti-Caspase-3, anti-Caspase-3 cleaved, and actin using the ECL chemiluminescence detection kit (Amersham, Arlington Heights, FL).

Nuclear Translocation Assay

The yellow fluorescent protein (YFP)-AR plasmid was donated by Marc I. Diamond (University of California, San Francisco, CA) and was stably transfected into HEK293 cells. Cells were seeded at 1.5×10^5 cells/cm^2 in optical microplates in phenol red-free DMEM/F12 medium supplemented with 10% hormone-depleted FBS. After 2 days of cultivation, the cells were pre-treated with enzalutamide (1 μM) or bicalutamide (1 μM) for 2 hr and then co-treated with 1 nM DHT for 1 hr in the presence of enzalutamide or bicalutamide. Cells were then washed in phosphate-buffered saline, incubated with the nuclear fluorescent marker DAPI (1 μg/ml) for 30 min and fixed with 4% paraformaldehyde for 30 min at room temperature. Cells were visualized using a Qimaging digital camera coupled to an Olympus X71 fluorescence microscope using a YFP filter (Chroma U-N31040). Nuclear and total cellular AR-YFP fluorescence intensities (integrated density) were quantified using ImageJ software (Version 1.46, National Institutes of Health, Bethesda, MD). Nuclear AR-YFP fluorescence was quantified in areas defined by image segmentation based on DAPI fluorescence, and the nuclear:total intensity ratio calculated. At least 14 cells were quantified per condition per independent experiment (n = 3). For live cell imaging experiments, cells were pre-treated with enzalutamide (1 or 10 μM) or bicalutamide (1 or 10 μM) for 2 hr and then co-treated with 1 nM DHT for 3 hr in the presence of enzalutamide or bicalutamide. Cells were imaged immediately before DHT addition ($t' = 0$) and then at 60-min intervals over 3 hr.

A β-galactosidase (β-gal) enzyme fragment complementation (EFC)-based assay, PathHunter NHRPro Nuclear Translocation assay (Discoverex, Fremont, CA), was used to monitor AR nuclear translocation [28]. In this β-galactosidase (βgal) EFC-based assay, wild type AR is recombinantly fused to a short inert fragment of βgal, termed prolabel, and an enzyme acceptor (EA, a large inert fragment of βgal), is fused to a nuclear location sequence that directs the expression of vEA to the nucleus. This construct was expressed in HEK293 cells. Migration of the ProLabel-tagged AR to the nucleus results in complementation with EA generating an active β-Gal enzyme and production of chemiluminescent signal. PathHunter NHRPro HEK293-AR cell lines were expanded according to standard procedures and maintained in selective growth media. Prior to assay, the cells were seeded into white walled clear bottom 384-well microplates at a density of 10,000 cells per well and allowed to adhere and recover overnight prior to compound addition in charcoal-dextran filtered media. For compound profiling in the agonist mode, cells were incubated in the presence of compound at 37°C for 5 hr. After incubation with the compounds, assay signal was generated through a single addition of PathHunter detection reagent cocktail for agonist and antagonist assays, respectively, followed by 1 hr incubation at room temperature. Microplates were read following signal generation with a PerkinElmer View-Lux™ instrument for chemiluminescent signal detection. Dose–response curves were plotted using GraphPad Prism.

Microarray Analysis

LNCaP cells were grown in RPMI 1640 supplemented with 5% hormone depleted FBS and treated with DHT and drug. RNA was extracted as described above (qPCR). Affymetrix U133 P2 array screening was developed according to the standard protocols of Asuragen, Inc. (Austin, TX) and data were analyzed with the SSP package. All microarray experiments were done in triplicate. Summarization of gene values was done using MAS 5.0, with all arrays scaled to 500 using Affymetrix GeneChip Operating Software. Gene annotation was obtained from Affymetrix Netaffx. Significant differences hypothesis testing was using one-way analysis of variance (ANOVA) or t-test as appropriate, with the false discovery rate set to 0.05. Data has been deposited into GEO database (accession no. GSE44905).

Mouse Xenograft Model

Following a 5-day acclimation period, 5- to 9-week-old male CB17SCID mice (Charles River Laboratories, Hollister, CA) were castrated and allowed to recover for an additional 5 days before inoculation with tumor cells. LNCaP cells co-expressing exogenous AR and the AR-dependent reporter construct ARR2-Pb-Luc (LNCaP-AR-Lux cells, a gift from Charles Sawyers, Memorial Sloan Kettering Cancer Center, New York, NY) were used to generate a xenograft model of human prostate cancer. Before implantation, LNCaP-AR-Lux cells were prepared by the addition of trypsin-EDTA, washed with complete medium, collected and resuspended at 20×10^6 cells/ml. Cell suspensions were diluted with Matrigel to 2×10^6 cells/0.2 ml and delivered subcutaneously in the suprascapular region. Tumor growth was monitored to the volume of 100 mm^3 when treatment began (~80 days). The observed rate of tumor take with LNCaP-AR-Lux cells is between 70% and 80%. Body weight and tumor volumes (width$^2 \times$ length/2) were measured two to three times per week with a digital caliper, and the average tumor volumes were determined. Test drugs were diluted in Tween 80: PEG 400, and stored at 4°C until administration by oral gavage. Each group of mice (n = 7) was treated daily for 28 consecutive days with 1, 10, or 50 mg/kg enzalutamide, vehicle control, or 50 mg/kg bicalutamide. At the end of the treatment period or when tumor volume exceeded 1,000 mm^3, animals were euthanized and blood and tissue samples were collected for analysis. All animal procedures were approved by institutional Animal Care and Use Committees.

Immunohistochemical Analysis

Tumor tissue samples were fixed in 10% neutral buffered formalin for 24 hr, transferred to 70% ethanol, and embedded in paraffin. A 4-μm section was stained with hematoxylin and eosin and evaluated for tumor necrosis or was immunohistochemically stained for proliferating cells with a monoclonal mouse Ki-67 (MIB-1) antibody (Dako, Carpinteria, CA). Pretreatment of heat-induced epitope retrieval in 10 mmol/L citrate buffer pH 6.0 was used for the Ki-67 antibody before the primary antibody incubation. Antibody was incubated for 30 min at room temperature and visualized using Envision + Mouse (Dako) followed by DAKO Liquid DAB+ and counterstained with hematoxylin. Digital images of the same relative area of each tumor of hematoxylin/eosin and Ki67 stained sections were captured with a Zeiss Axiocam HRC HR Digital Camera and Axiovision software release 4.4.

RESULTS

Enzalutamide Inhibits Androgen-Dependent Gene Expression (PSA mRNA) in CRPC Cell Culture Models

To assess the antagonistic and agonistic properties of enzalutamide and bicalutamide on AR target gene expression, LNCaP prostate cancer cells and the LNCaP-derived androgen-independent C4-2 cell lines were treated in the presence and absence of DHT. Transcript levels of the AR target gene *KLK3*, which encodes for the PSA, and *TMPRSS2* (transmembrane protease serine 2) were evaluated by quantitative real-time PCR (Fig. 1, Supplementary Fig. 1). Enzalutamide alone did not induce gene expression of *KLK3* or *TMPRSS2* (Fig. 1A, Supplementary Fig. 1A). As seen previously, bicalutamide behaved as an agonist of androgen-dependent gene expression [29–31] significantly inducing the expression of PSA and *TMPRSS2* at concentrations ≥10 μM (Fig. 1A, Supplementary Fig. 1A). Both enzalutamide and bicalutamide significantly antagonized the induction of PSA expression by DHT (Fig. 1B). However, enzalutamide was effective at lower concentrations than bicalutamide. Enzalutamide and bicalutamide also inhibited agonist-induced expression of *TMPRSS2* (Supplementary Fig. 1B). In C4-2 cells, bicalutamide (10 μM) induced PSA mRNA levels whereas enzalutamide (10 μM) did not (Fig. 1C). Enzalutamide significantly antagonized DHT-induced PSA mRNA expression at 10 μM. In contrast, 20 μM bicalutamide was necessary to inhibit PSA expression to a similar degree (Fig. 1D). No effects on the housekeeping gene human α 4^a tubulin were observed in any condition.

Enzalutamide Inhibits AR Nuclear Translocation

It has been reported that micromolar concentrations of bicalutamide agonistically increase AR nuclear
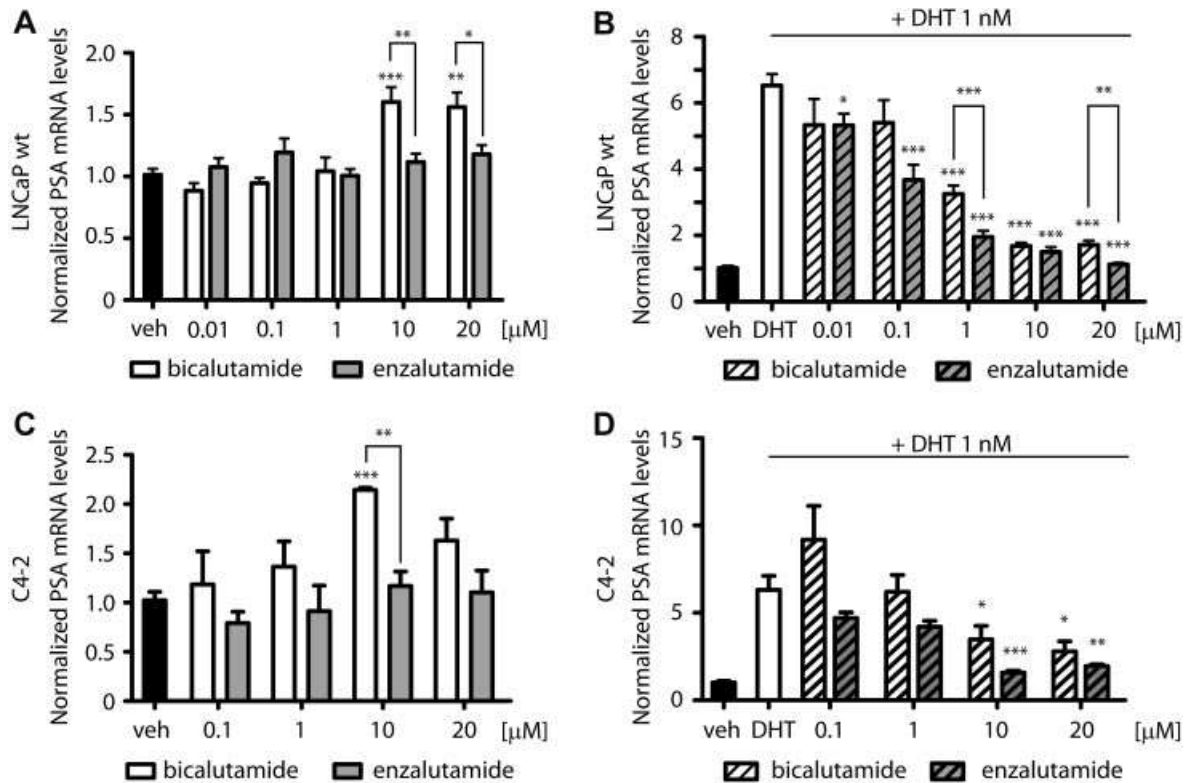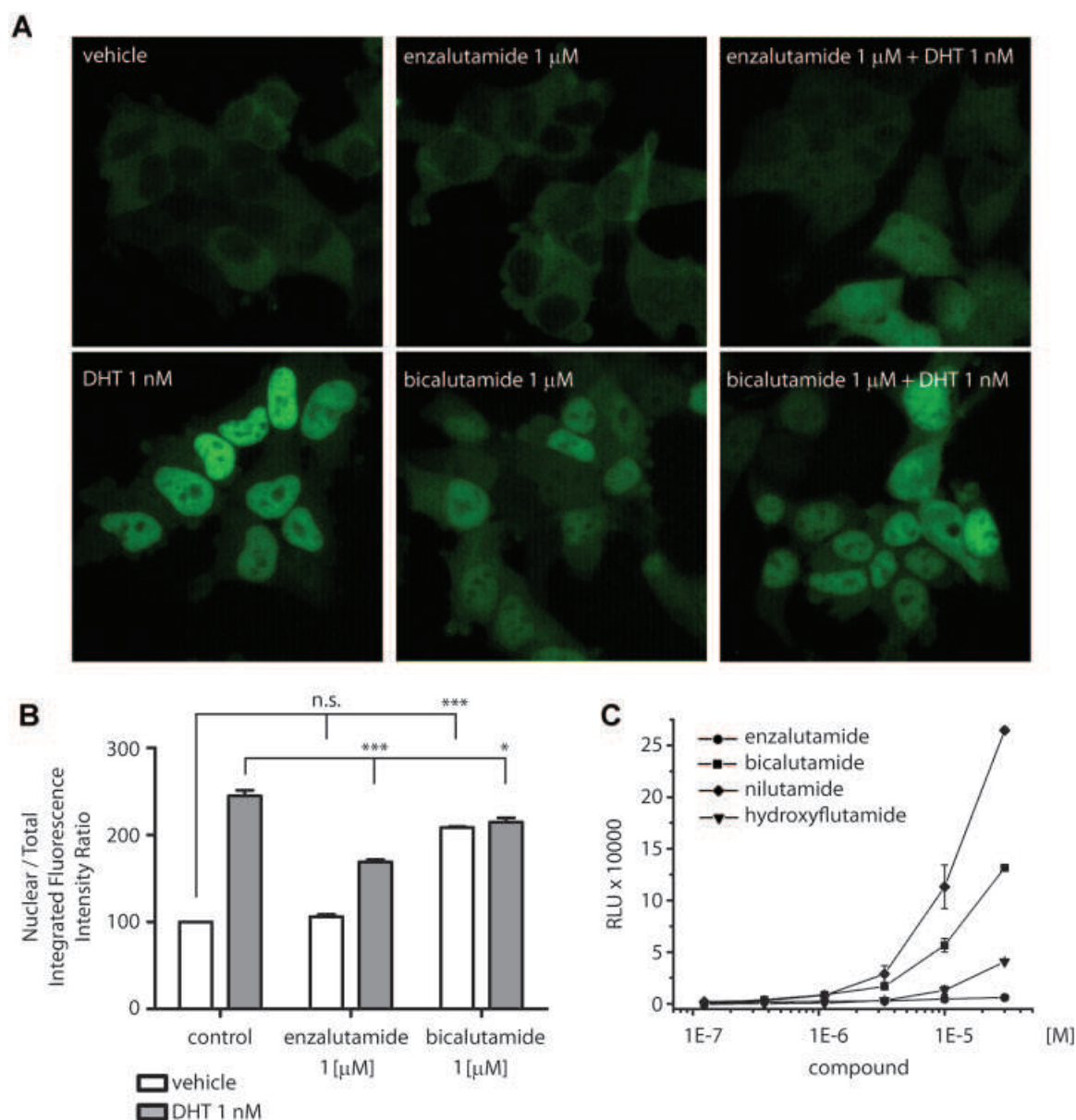
Fig. I. Enzalutamide inhibits agonist-induced transcription of the AR-dependent gene prostate-specific antigen. PSA mRNA levels in wild-type LNCaP (LNCaP-wt) (A and B) and C4-2 cells (C and D) were measured by qRT-PCR. Cells were treated for 8 hr with DMSO (vehicle), enzalutamide alone or bicalutamide alone (A and C) or enzalutamide or bicalutamide in the presence of I nM of DHT (B and D). Data were normalized to expression levels of α-tubulin and the value of PSA expression in vehicle-treated cells was set to I.0. Data are displayed as mean $\pm$ SEM (error bars), n = 6 ($^{***}P < 0.001$, $^{**}P < 0.01$, $^{*}P < 0.05$, each treatment was tested individually against vehicle using the Student's t-test).

translocation, AR binding to DNA, and transcription of AR-responsive genes [25,32]. In contrast, enzalutamide, which has been proposed to function as a pure AR antagonist, has been shown to inhibit AR nuclear translocation and DNA binding [25]. To evaluate the effects of enzalutamide and bicalutamide on AR nuclear translocation, the nuclear distribution of AR was determined in HEK293 cells stably transfected with a wild-type AR-YFP construct and treated with drug in the presence and absence of DHT 1 nM (Fig. 2A). Nuclear versus total fluorescence intensity ratios of AR-YFP were quantified as indicated in Materials and Methods Section and normalized against values obtained from vehicle-treated cells (Fig. 2B). Bicalutamide treatment at 1 µM increased the relative nuclear AR-YFP fluorescence intensity compared with vehicle-treated cells (Fig. 2B). In contrast, 1 µM enzalutamide treatment had no effect on the nuclear-to-total ratio of AR-YFP fluorescence intensity (Fig. 2B). The agonistic and antagonistic effects of the drugs were confirmed in live single cell imaging of HEK293 AR-YFP cells over time (Supple-

mentary Fig. 2). Pretreatment with 1 or 10 µM bicalutamide for 30 min clearly induced agonistic AR translocation in the absence of DHT (Supplementary Fig. 2B and C, $t' = 0$, arrowheads). In contrast, no agonistic effects were observed with pre-treatment of 1 µM enzalutamide (Supplementary Fig. 2D, $t' = 0$). In general, cells pre-treated with 10 µM enzalutamide-displayed diffuse AR-YFP staining between the nucleus and cytoplasm in the absence of DHT. In the presence of DHT, a slight response was detected in a few isolated cells (see arrowheads, Supplementary Fig. 2E, $t' = 0$).

To characterize in more detail the agonistic effects of enzalutamide and the antiandrogens bicalutamide, nilutamide, and hydroxyflutamide on AR nuclear translocation, dose–response profiles for each compound were evaluated using a cell-based chemoluminescent β-gal complementation assay (Fig. 2C) [28]. Nilutamide and bicalutamide stimulated AR translocation at micromolar concentrations and hydroflutamide (>10 µM) induced agonistic effects on AR translocation (Fig. 2C). Enzalutamide alone did not

Fig. 2. Enzalutamide inhibits agonist-induced nuclear translocation of AR. A: Representative fluorescence microscopy images of nuclear translocation of AR in HEK-293 cells expressing AR-YFP. Cells were treated with DHT (1 nM) alone, enzalutamide or bicalutamide alone and DHT + enzalutamide or bicalutamide. B: Quantification of the ratio of integrated fluorescence intensities of AR-YFP in the nucleus versus the total cell. Values correspond to means of measurements from three independent experiments where at least 14 cells were quantified for each treatment (vehicle, 1 μM enzalutamide, 1 μM bicalutamide, 1 nM DHT, and 1 nM DHT + 1 μM enzalutamide or bicalutamide). Values were normalized to the vehicle and tested for statistical significance ($^{***}P < 0.001$, $^{**}P < 0.01$, $^{*}P < 0.05$, one-sample and student's t-tests). C: Dose−response curves for AR nuclear translocation induced by enzalutamide (●), bicalutamide (■), nilutamide (◆), or hydroxyflutamide (▼) alone. The fraction of AR receptor that translocates to the nucleus was measured using PathHunter NHRPro AR nuclear translocation cell lines (RLU, relative luminescence units).

induce AR nuclear translocation at any concentration evaluated (≤30 μM). 6-α-Fluorotestosterone was used as a control to stimulate AR nuclear translocation (Supplementary Fig. 3). These results indicate that enzalutamide is more effective than the antiandrogens analyzed at inhibiting AR-nuclear translocation in the presence of the agonist DHT. Moreover, compared with bicalutamide, nilutamide, or hydroxyflutamide, enzalutamide showed no agonistic effects with respect to AR nuclear translocation.

In summary and consistent with previous studies [25], we found that there was no evidence of enzaluta-

mide agonist behavior in AR target gene expression in multiple CRPC cell models and that enzalutamide does have antagonistic activity in agonist-induced androgen-dependent signaling. Furthermore, these results indicate that in vitro, enzalutamide is more potent than bicalutamide as an inhibitor of AR-dependent signaling.

Enzalutamide Treatment Decreased Tumor Volume, Increased Body Weight, and Induced Apoptosis in a Mouse LNCaP-AR Xenograft Model

To study the effects of enzalutamide and bicalutamide in vivo, a mouse xenograft CRPC model was developed using castrated male animals implanted with human LNCaP-AR cells that over-express wild-type AR [25]. Animals were administered enzalutamide (1–50 mg/kg/day) or bicalutamide (50 mg/kg/day), and tumor volume and mouse body weight were measured at 2- to 3-day intervals for 28 days. Bicalutamide (50 mg/kg/day) inhibited tumor growth through Day 16 when compared with the vehicle control group. After Day 16, however, tumors in these mice grew continuously up to 154% of baseline by Day 28 (Fig. 3A, Table I). In contrast, enzalutamide (10 mg/kg/day) inhibited tumor growth significantly during the first 6 days of treatment compared with vehicle- and bicalutamide-treated mice (mean $\pm$ SE percentage tumor growth relative to baseline: vehicle, $119 \pm 5\%$; enzalutamide 10 mg/kg, $86 \pm 6\%$, bicalutamide 50 mg/kg, $106 \pm 8\%$). By Day 13, enzalutamide treatment resulted in a 19% decrease in tumor volume at doses of 10 mg/kg/day or greater compared with the initial tumor size (Fig. 3A). Some tumors in the enzalutamide-treated groups (1 and 50 mg/kg) decreased in size significantly so as to be beyond the measurement limits (Table I, non-measurable tumors/group). These tumors were not included in further analysis. Tumor volume continued to decrease through Day 24 for the 10 mg/kg/day-enzalutamide group and through the last measured time point at Day 28 for the 50-mg/kg/day group (Table I). Maximal effect on tumor regression relative to initial tumor volumes in each group occurred at Day 28 or beyond of enzalutamide treatment (Fig. 3A). The mean $\pm$ SE relative tumor volume decline after 27 days of enzalutamide treatment was $41 \pm 7\%$ at 10 mg/kg and $68 \pm 13\%$ at 50 mg/kg compared with baseline. In contrast, after 27 days of vehicle or 50 mg/kg bicalutamide treatments, tumor volume increased 54% when compared with the baseline (Table I).

Change in mouse body weight was also used to assess gross toxicity. Enzalutamide appeared to have a positive effect resulting in increased body weight (Fig. 3B). Over the 28 days of treatment, enzalutamide at 10
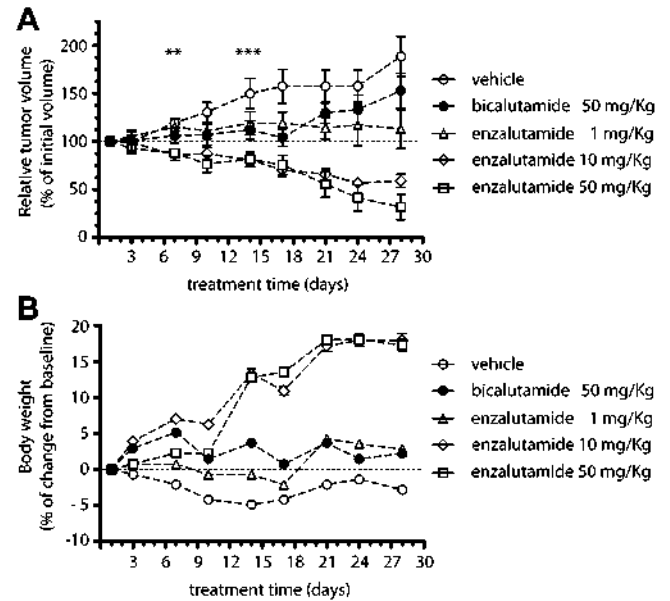
Fig. 3. Enzalutamide reduces tumor volume in a human LNCaP-AR xenograft model. A: Tumor volume changes of mice treated by oral daily gavage with vehicle, bicalutamide or enzalutamide for 28 days. Data were graphed as tumor volumes (mm^3) and error bars represent standard error. Days of treatment in which differences of tumor volume compared to initial volume reach significance are indicated for enzalutamide 10 mg/kg treatment group ($^{**}P < 0.01$, $^{****}P < 0.001$, nonparametric ANOVA with Kruskal–Wallis post test). B: Body weight changes of mice treated by oral daily gavage with vehicle, bicalutamide or enzalutamide for 28 days. Weights are plotted as the differences from the starting weights of the mice and these differences are normalized to the starting weights. Data points reflect the mean of relative body weight changes, respectively, and error bars represent the standard deviation (n = 7 mice per group). All data points in (A) and (B) are plotted with error bars, some of which are too small to be visible.

and 50 mg/kg resulted in body weight increases of 8.5% and 12.1%, respectively, compared with baseline, indicative of healthy mice. At the lower enzalutamide dose (1 mg/kg), body weights were comparable to those from the vehicle-treated group (Fig. 3B, Table II).

Immunohistochemical analysis of staining for Ki67, a marker of cell proliferation, in LnCaP-AR xenograft tissue revealed a decrease in cell proliferation in enzalutamide-treated mice compared with vehicle-treated mice (Fig. 4B). Additionally, enzalutamide treatment induced cell apoptosis, as determined by an increase in activated Caspase-3 levels in LNCaP-AR cells treated with 1 or 10 μM enzalutamide (Fig. 4C). In comparison, no activation of Caspase-3 was seen in vehicle-treated cells. Taken together these results indicate that enzalutamide-mediated inhibition of AR signaling induces cell apoptosis and contributes to the inhibition of tumor growth and tumor volume regression overtime.

TABLE I. Tumor Growth in Human LNCaP-AR Xenograft Model in Mice Treated With Enzalutamide or Bicalutamide

Treatment group	Non-measurable tumors/group	Day 0		Day 28	
		Mean $\pm$ SD tumor volume, mm^3	Mean $\pm$ SD tumor volume, mm^3	Mean $\pm$ SE change in tumor volume, %	Mean tumor volume regression, %
Vehicle control	0/7	176 $\pm$ 65	348 $\pm$ 192	+89 $\pm$ 21	—
Enzalutamide, 1 mg/kg/day	1/7	170 $\pm$ 41	202 $\pm$ 98	+13 $\pm$ 20	—
Enzalutamide, 10 mg/kg/day	0/7	212 $\pm$ 91	132 $\pm$ 93	−59 $\pm$ 7	41.1
Enzalutamide, 50 mg/kg/day	3/7	193 $\pm$ 85	62 $\pm$ 65	−32 $\pm$ 13	68.3
Bicalutamide, 50 mg/kg/day	0/7	206 $\pm$ 67	330 $\pm$ 198	+54 $\pm$ 18	—

Differential Microarray Gene Expression Analysis of LNCaP Cells in Response to DHT and Enzalutamide

Affymetrix human genome U133 2.0 Array technology was used to determine the effects of enzalutamide treatment on the transcriptional profile of prostate cancer cells. LNCaP cells were treated with vehicle, DHT (100 nM), or enzalutamide (1 or 10 μM) for 16 hr. Each condition was done in triplicate. Principal component analysis (PCA) and non-supervised hierarchical clustering (Supplementary Fig. 4) of the gene expression data from each array were performed to test the reproducibility of the experimental design. PCA, performed on genes differentially expressed in test conditions compared with the vehicle control (ANOVA, $P < 0.05$), illustrated that the replicate experiments gave highly reproducible results and that there were clear differences in gene expression between test conditions (Supplementary Fig. 4A). The hierarchical clustering of gene expression profiles also demonstrated the high reproducibility of the assay because the three replicates of each treatment group clustered tightly together (Supplementary Fig. 4B). Additionally, cells treated with 1 or 10 μM enzalutamide displayed similar gene expression patterns suggesting that the changes in the gene expression profile

induced by enzalutamide treatment are independent of dose (Supplementary Fig. 4B).

To determine the effects of enzalutamide on DHT-induced gene expression, it was first determined which genes were affected by DHT alone compared with vehicle. All results were filtered for statistical significance (t-test, $P < 0.05$). A total of 2,539 genes were found to be differentially regulated by DHT alone compared with the vehicle-treated condition (Table III). As expected, AR target genes, such as *KLK2*, *IGF1R*, *FKBP5*, *NKX3.1*, and *TMPRSS2* [33], were in this group. The effects of enzalutamide treatment on the expression of these genes were determined by quantifying the differences in expression in cells treated with DHT + enzalutamide (1 or 10 μM) compared with DHT alone. Of the 2,539 DHT-regulated genes, 599 (23.6%; 223 up-regulated, 376 down-regulated) were regulated in an opposite manner in the cells treated with 1 μM enzalutamide + DHT than in cells treated with DHT alone (Fig. 5A and B, Table III). All of these 599 genes maintained a similar expression pattern in response to treatment with DHT + 10 μM enzalutamide (Fig. 5A and B, Table III). Therefore, genes whose expression increased upon DHT treatment were downregulated in cells treated with DHT + enzalutamide (1 or 10 μM). Furthermore, most of these (475 of 599) displayed dose-

TABLE II. Body Weight Values of Human LNCaP-AR Xenograft Model in Mice Treated With Enzalutamide or Bicalutamide

Treatment group	No. mice (n)	Mean body weight (g) mean $\pm$ SD		% Body weight gain
		Day 0	Day 28	
Vehicle control	7	20.4 $\pm$ 2.2	19.9 $\pm$ 2.0	—
Enzalutamide, 1 mg/kg/day	7	20.1 $\pm$ 2.7	20.7 $\pm$ 2.7	4
Enzalutamide, 10 mg/kg/day	7	18.3 $\pm$ 1.8	21.6 $\pm$ 1.6	8.5
Enzalutamide, 50 mg/kg/day	7	19 $\pm$ 1.6	22.3 $\pm$ 1.5	12.1
Bicalutamide, 50 mg/kg/day	7	19.4 $\pm$ 1.7	19.9 $\pm$ 1.9	0
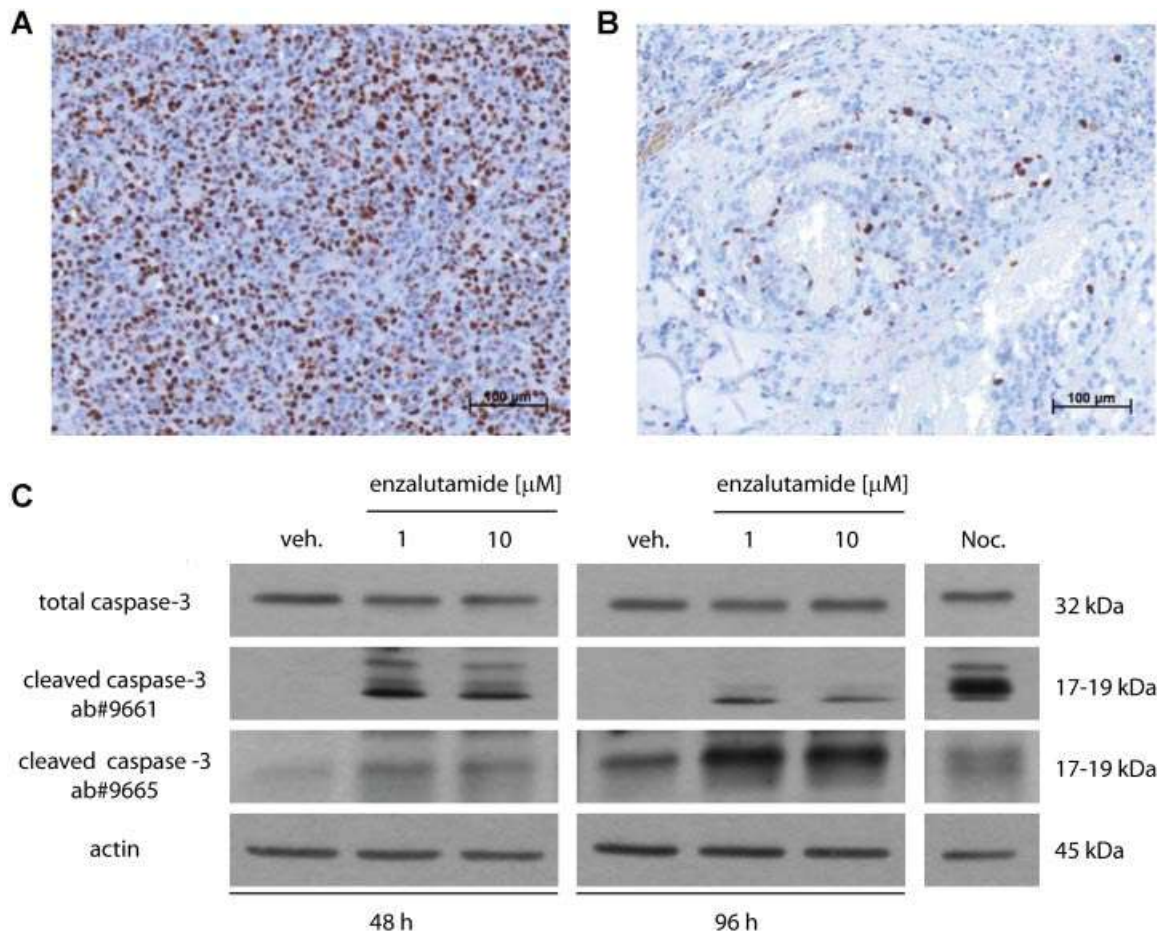
Fig. 4. Enzalutamide induces apoptotic cell death and tumor shrinkage in mouse xenograft models. A and B: Immunohistochemical staining of Ki67 in the LNCaP-AR xenograft model. Mice were treated by oral daily gavage with vehicle (A) or enzalutamide 10 mg/kg (B) for 7 days. C: Western blot analysis of the apoptotic marker cleaved Caspase-3 in LNCaP-AR cells. Cells were treated with enzalutamide (1 and 10 µM) for 2 or 4 days; 1 µg/ml nocodazole (Noc.), which induces apoptosis, was used as positive control.

dependent changes: the magnitudes of the expression differences seen between treatment with drug + DHT and DHT alone augmented with increased drug concentration (Fig. 5A and B, Table III). In total, 52%, 1321 of 2539 genes affected by DHT alone (615 up-regulated, 706 down-regulated) were differentially regulated in cells treated with 10 µM enzalutamide

and DHT (Table III) illustrating that a higher concentration of enzalutamide differentially affects a greater number of AR-regulated genes.

The biological pathways, processes, and molecular functions represented by the genes differentially expressed in response to enzalutamide in LNCaP cells were analyzed using the online functional gene anno-

TABLE III. Summary of Microarray Expression Analysis in LNCaP Cells Treated With DHT and Enzalutamide

		Genes regulated significantly			Genes with ≥twofold changes	
Treatment	Compared to	Total	Up-regulated	Down-regulated	Up-regulated	Down-regulated
DHT, 100 nM	VEH	2,539	1,199	1,340	398	415
Enzalutamide, 1 M	VEH	203	78	125	13	20
Enzalutamide, 10 M	VEH	262	113	149	16	16
DHT + enzalutamide, 1 M	DHT	599	223	376	42	126
DHT + enzalutamide, 10 M	DHT	1,321	615	706	131	244
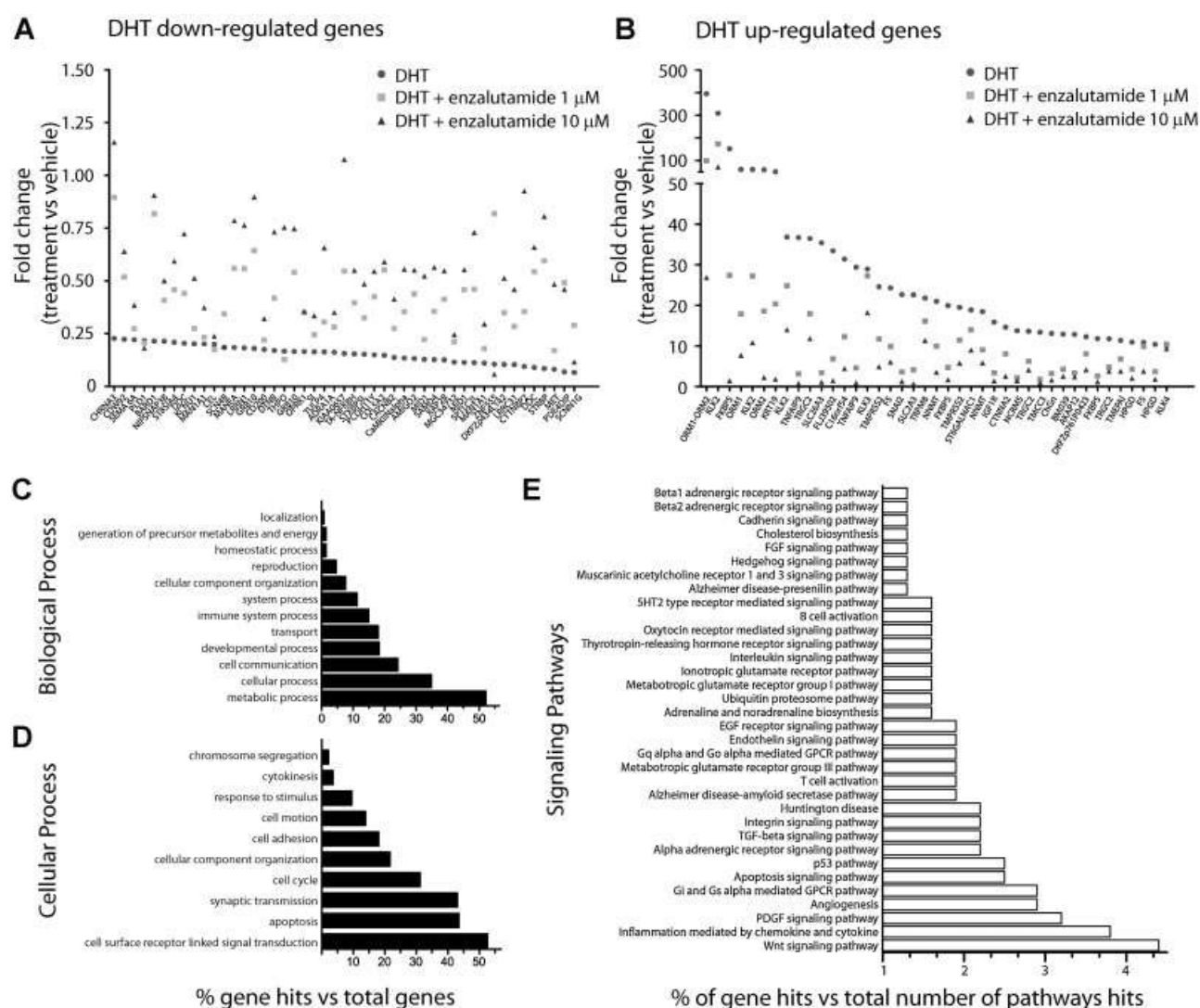
Fig. 5. Summary of microarray analysis. A and B: Expression ratio (fold change) for the list of 40 genes with more significant differential expression between DHT versus vehicle (●), DHT + 1 μM enzalutamide versus vehicle (■) and DHT + 10 μM enzalutamide versus vehicle (▲). Data are presented for genes significantly down-regulated with DHT (A) and significantly up-regulated by DHT (B). C–E: Summary graphs of biological processes (C), cellular processes (D), and signaling pathways (E) represented by the genes differentially expressed by enzalutamide in comparison with DHT according to PANTHER analysis. Overrepresented ontology terms belonging to the biological and cellular processes categories were graphed as the percentage of gene hits against total number of genes (C and D). Overrepresented signaling pathways (over 1%) were graphed as the percentage of gene hits against the total number of pathways.

tation platform PANTHER, a classification system and database of protein families [34] (Fig. 5C–E). Of the 1,321 genes differentially regulated in the presence of enzalutamide + DHT, 773 were successfully mapped in the PANTHER gene ontology database. The cellular processes and biochemical pathways whose components were over-represented in this group of genes, such as apoptosis, cell adhesion, Wnt signaling, and the p53 pathway (see Fig. 5D and E for full lists), are well known to be involved in the development or progression of cancer. However, they have not been

associated previously with enzalutamide activity in prostate cancer cells.

To determine which genes had the largest changes in expression, the data were filtered for changes in expression of twofold or greater between enzalutamide + DHT (1 or 10 μM) versus DHT alone. The 375 (12.8%) and 168 (5.8%) genes, respectively, were differentially expressed to such a degree (Supplemental Data, Table SI). In the presence of DHT and 10 μM enzalutamide, 131 genes were up-regulated and 126 genes were down-regulated differentially compared

with DHT alone, and 99 of these genes (29 up-regulated and 70 down-regulated genes) showed a dose–response pattern in response to enzalutamide (Supplemental Data, Table SI). Among the genes with a direct dose–response pattern were genes that have been found previously to be related to cancer. For example, the group of genes up-regulated on treatment with enzalutamide + DHT (and down-regulated in DHT treatment) includes tumor suppressors such as the Cub and Sushi multiple domains-1 protein [35] and the BRCA1-associated RING domain 1 protein [36,37] (Supplemental Data, Table SI). As expected, genes that were down-regulated in a dose-dependent manner by at least twofold in the presence of enzalutamide + DHT compared with DHT alone included components of signaling pathways that have been associated with CRCP, such as the serum/glucocorti-coid-regulated kinase 1 [38], the leukemia inhibitory factor receptor [39,40], the insulin growth factor receptor 1, and the FK506 binding protein 5 (FKBP5) [41] (see Supplemental Data, Table SI for a full list).

DISCUSSION

In this work, we evaluated the effects of the novel ARSI enzalutamide on the inhibition of AR signaling and cell growth in different human CRPC cell models. Recent evidence has led to the consensus that AR-dependent signaling is involved in the development and progression of prostate cancer. Increased AR signaling due to over-expression of the receptor and up-regulation of signaling pathways that feed into the AR pathway have been shown to contribute to the development of androgen insensitive AR signaling and resistance [7–11,17,42]. Similarly, mutations in the AR LBD present in human CRPC tumors after classical androgen deprivation create an AR that is more sensitive to androgen levels and responds to non-androgen hormone ligands [15]. Antiandrogens (e.g., bicalutamide) have proven to be inefficient in sustained CRPC treatment and have been shown to have agonistic activity on AR signaling in prostate cancer cell lines that over-express AR [7,15–17,32] or harbor the W741C mutation in the LBD of AR [43,44]. In agreement with other studies [29–31], higher bicaluta-mide concentrations (>10 μM) were found to induce a significant increase in PSA mRNA expression in LNCaP cells, which express normal levels of AR. In contrast, cells treated with up to 20 μM enzalutamide displayed no agonistic increases in AR target gene expression.

In response to androgen binding, the AR undergoes an intramolecular interaction between the N-terminal FxxLF motif (^{23}FQNLF^{27}) and the AF2 surface domain in the LBD on the C-terminal (N/C intramolecular interaction) that stabilizes the AR-ligand complex before the transport to the nucleus [45–48]. Localization of the AR-complex depends on an intricate equilibrium between the interactions of the importin α/β and Ran GTP-ase nuclear import system [49] with the nuclear localization signals located in the N-terminal transactivation domain (NTD), the DNA-binding domain, and the LBD [49,50]. AR localization is also affected by the interactions between the cellular nuclear export systems and the nuclear export signals located in the LBD [50–52] and cytoplasm retention signals located in the NTD and LBD domains of AR. Exposure of signals in AR to localization machinery is modulated in response to androgen ligand binding [49,53]. Antiandrogens such as bicalutamide are able to competitively bind to AR in the LBD and inhibit the agonist dependent N/C-terminal intramolecular inter-action [54]. This can promote the assembly of a transcriptionally inactive receptor by inhibiting coactivator binding [55,56] or promoting corepressor association [45,57]. However, bicalutamide does not prevent AR nuclear translocalization nor binding to AR-complex responsive elements in chromatin [56]. At micromolar concentrations, enzalutamide is able to inhibit androgen-induced AR nuclear translocation and in contrast to bicalutamide and other antiandrogens, does not stimulate AR translocation, suggesting a mechanism where enzalutamide binds to AR and locks it in a translocation-defective conformation that potently inhibits AR nuclear translocation in response to androgens.

LNCaP and C4-2 cells carry the T877A gain of function mutation in the LBD but this mutation has been shown to have little or no effect on the binding of bicalutamide [22,58]. The partial agonist activity of bicalutamide is also unaffected by this mutation [59]. While it is not clear what effect the T877A mutation may have on the binding or efficacy of enzalutamide, our results indicates that when compared side-by-side, enzalutamide displays lower agonist activity and is a more effective antagonist than bicalutamide. Similar results were found in HEK-293 cells overexpressing wild type AR as measured by the nuclear translocation of AR. Although we cannot discard the possibility that the T877A mutation could differentially affect the two drugs, these data suggest that enzalutamide is a weaker AR agonist than bicalutamide.

The lack of agonist activity of enzalutamide at concentrations that bicalutamide displays agonist activity may be expected to be due to differences in AR-binding affinities. However, the relative binding affinities of the two drugs for wild-type AR [25] do not correlate with the differences in their agonistic effects on AR nuclear translocation. Bicalutamide binds less tightly to AR than enzalutamide but has more agonist

activity. Finally, the observed agonistic effects of other known AR antagonists on AR nuclear translocation suggest that there is no relationship between relative binding affinity and the stimulatory effects antiandrogens on AR transport [60]. Recent evidence indicates that agonistic responses of anti-androgens on mutant AR receptors are independent of antagonist-binding affinities, and it has been suggested that the antagonist-induced rearrangement of AR into a transcriptionally active agonist conformation could play a role [61]. Alternatively, the differential association of mutant receptors with co-regulators [58,62] or the association of AR with androgen responsive elements in the DNA [63] may affect the agonist activity of drugs. The absence of AR agonism of enzalutamide is a particular property of this molecule independent of its antagonistic binding activity and may be responsible the greater inhibition of DNA binding and transcriptional activity of AR, as compared to other known AR antagonists.

The most striking result of enzalutamide treatment is its capacity to not only arrest tumor growth, but to decrease tumor volume overtime. As was reported previously [25], enzalutamide treatment causes a regression of tumors in a CRPC xenograft model in vivo. The data reported here show that enzalutamide induces cell apoptosis in prostate cancer cells over-expressing AR, suggesting a mechanism that could contribute to the reduction in tumor volume. Additionally, these data could provide an explanation for the 28.9% increase in overall survival of enzalutamide-treated patients in the phase 3 placebo controlled trial (AFFIRM, NCT00974311) [26]. In contrast, bicalutamide treatment initially induced tumor growth inhibition in the xenograft model, but the effect was not sustained and tumors resumed growing at the same rate as in untreated animals. Several mechanisms of cell apoptosis have been associated with AR signaling down-regulation [64].

Microarray analysis of the effects on gene expression of treatment of LNCaP cells with enzalutamide in the presence of DHT revealed 1,321 genes that were significantly regulated by enzalutamide compared with DHT alone. These androgen responsive genes include tumor suppressors, genes associated with progression and survival of CRPC cells, and the regulation of AR signaling. These changes in gene expression induced by enzalutamide treatment could lend further support to a mechanism by which it causes tumor regression and apoptosis and could also be important for explaining the increased survival with enzalutamide in prostate cancer after chemotherapy in advanced CRPC patients [26]. Recently, it has been shown that AR and glucocorticoid receptor (GR) cistromes and transcription programs exhibit significant overlap in prostate cancer cells [65]. Additionally,

GR regulates a large number of genes considered to be AR pathway-specific [65]. This raises questions about the role of GR in the progression of prostate cancer under castration-resistant and androgen-deprived conditions. Interestingly, men with CRPC treated with abiraterone are likely to be treated also with glucocorticoids (prednisone or dexamethasone) to inhibit ACTH secretion induced by adrenal steroid synthesis. Further studies are needed to elucidate if enzalutamide can also regulate GR transcriptional program in CRPC.

CONCLUSIONS

These results suggest that the molecular effects of enzalutamide on AR signaling and gene expression contribute to its effectiveness in treating CRPC and represent mechanistic advantages of enzalutamide over antiandrogens. Enzalutamide is the first therapy targeting multiple events in the AR signaling pathway that has demonstrated increased overall survival in a placebo-controlled clinical trial in patients with CRPC [26]. These results support the use of enzalutamide as a therapeutic agent in patients with prostate cancer where AR signaling persists.

ACKNOWLEDGMENTS

REFERENCES

1. Shelke AR, Mohile SG. Treating prostate cancer in elderly men: How does aging affect the outcome? Curr Treat Options Oncol 2011;12(3):263–275.

2. Dutt SS, Gao AC. Molecular mechanisms of castration-resistant prostate cancer progression. Future Oncol 2009;5(9):1403–1413.

3. Lamont KR, Tindall DJ. Androgen regulation of gene expression. Adv Cancer Res 2010;107:137–162.

4. Jenster G. The role of the androgen receptor in the development and progression of prostate cancer. Semin Oncol 1999;26(4):407–421.

5. Devlin HL, Mudryj M. Progression of prostate cancer: Multiple pathways to androgen independence. Cancer Lett 2009;274(2):177–186.

6. Yuan X, Balk SP. Mechanisms mediating androgen receptor reactivation after castration. Urol Oncol 2009;27(1):36–41.

7. Chen CD, Welsbie DS, Tran C, Baek SH, Chen R, Vessella R, Rosenfeld MG, Sawyers CL. Molecular determinants of resistance to antiandrogen therapy. Nat Med 2004;10(1):33–39.

8. Koivisto P, Kononen J, Palmberg C, Tammela T, Hyytinen E, Isola J, Trapman J, Cleutjens K, Noordzij A, Visakorpi T, Kallioniemi OP. Androgen receptor gene amplification: A possible molecular mechanism for androgen deprivation therapy failure in prostate cancer. Cancer Res 1997;57(2):314–319.

9. Linja MJ, Savinainen KJ, Saramaki OR, Tammela TL, Vessella RL, Visakorpi T. Amplification and overexpression of androgen receptor gene in hormone-refractory prostate cancer. Cancer Res 2001;61(9):3550–3555.

10. Shiota M, Yokomizo A, Naito S. Increased androgen receptor transcription: A cause of castration-resistant prostate cancer and a possible therapeutic target. J Mol Endocrinol 2011;47:R25–R41.

11. Visakorpi T, Hyytinen E, Koivisto P, Tanner M, Keinanen R, Palmberg C, Palotie A, Tammela T, Isola J, Kallioniemi OP. In vivo amplification of the androgen receptor gene and progression of human prostate cancer. Nat Genet 1995;9(4):401–406.

12. Feldman BJ, Feldman D. The development of androgen-independent prostate cancer. Nat Rev Cancer 2001;1(1):34–45.

13. Hara T, Miyazaki J, Araki H, Yamaoka M, Kanzaki N, Kusaka M, Miyamoto M. Novel mutations of androgen receptor: A possible mechanism of bicalutamide withdrawal syndrome. Cancer Res 2003;63(1):149–153.

14. Veldscholte J, Voorhorst-Ogink MM, Bolt-de Vries J, van Rooij HC, Trapman J, Mulder E. Unusual specificity of the androgen receptor in the human prostate tumor cell line LNCaP: High affinity for progestagenic and estrogenic steroids. Biochim Biophys Acta 1990;1052(1):187–194.

15. Culig Z, Hoffmann J, Erdel M, Eder IE, Hobisch A, Hittmair A, Bartsch G, Utermann G, Schneider MR, Parczyk K, Klocker H. Switch from antagonist to agonist of the androgen receptor bicalutamide is associated with prostate tumour progression in a new model system. Br J Cancer 1999;81(2):242–251.

16. Hobisch A, Hoffmann J, Lambrinidis L, Eder IE, Bartsch G, Klocker H, Culig Z. Antagonist/agonist balance of the nonsteroidal antiandrogen bicalutamide (Casodex) in a new prostate cancer model. Urol Int 2000;65(2):73–79.

17. Kawata H, Ishikura N, Watanabe M, Nishimoto A, Tsunenari T, Aoki Y. Prolonged treatment with bicalutamide induces androgen receptor overexpression and androgen hypersensitivity. Prostate 2010;70(7):745–754.

18. Horoszewicz JS, Leong SS, Kawinski E, Karr JP, Rosenthal H, Chu TM, Mirand EA, Murphy GP. LNCaP model of human prostatic carcinoma. Cancer Res 1983;43(4):1809–1818.

19. Gaddipati JP, McLeod DG, Heidenberg HB, Sesterhenn IA, Finger MJ, Moul JW, Srivastava S. Frequent detection of codon 877 mutation in the androgen receptor gene in advanced prostate cancers. Cancer Res 1994;54(11):2861–2864.

20. Suzuki H, Akakura K, Komiya A, Aida S, Akimoto S, Shimazaki J. Codon 877 mutation in the androgen receptor gene in advanced prostate cancer: Relation to antiandrogen withdrawal syndrome. Prostate 1996;29(3):153–158.

21. Sun C, Shi Y, Xu LL, Nageswararao C, Davis LD, Segawa T, Dobi A, McLeod DG, Srivastava S. Androgen receptor mutation (T877A) promotes prostate cancer cell growth and cell survival. Oncogene 2006;25(28):3905–3913.

22. Veldscholte J, Berrevoets CA, Brinkmann AO, Grootegoed JA, Mulder E. Anti-androgens and the mutated androgen receptor of LNCaP cells: Differential effects on binding affinity, heat-shock protein interaction, and transcription activation. Biochemistry 1992;31(8):2393–2399.

23. Dehm SM, Tindall DJ. Ligand-independent androgen receptor activity is activation function-2-independent and resistant to antiandrogens in androgen refractory prostate cancer cells. J Biol Chem 2006;281(38):27882–27893.

24. Jung ME, Ouk S, Yoo D, Sawyers CL, Chen C, Tran C, Wongvipat J. Structure-activity relationship for thiohydantoin androgen receptor antagonists for castration-resistant prostate cancer (CRPC). J Med Chem 2010;53(7):2779–2796.

25. Tran C, Ouk S, Clegg NJ, Chen Y, Watson PA, Arora V, Wongvipat J, Smith-Jones PM, Yoo D, Kwon A, Wasielewska T, Welsbie D, Chen CD, Higano CS, Beer TM, Hung DT, Scher HI, Jung ME, Sawyers CL. Development of a second-generation antiandrogen for treatment of advanced prostate cancer. Science 2009;324(5928):787–790.

26. Scher HI, Fizazi K, Saad F, Taplin ME, Sternberg CN, Miller K, de Wit R, Mulders P, Chi KN, Shore ND, Armstrong AJ, Flaig TW, Flechon A, Mainwaring P, Fleming M, Hainsworth JD, Hirmand M, Selby B, Seely L, de Bono JS. Increased survival with enzalutamide in prostate cancer after chemotherapy. N Engl J Med 2012;367(13):1187–1197.

27. Schmittgen TD, Livak KJ. Analyzing real-time PCR data by the comparative C(T) method. Nat Protoc 2008;3(6):1101–1108.

28. Fung P, Peng K, Kobel P, Dotimas H, Kauffman L, Olson K, Eglen RM. A homogeneous cell-based assay to measure nuclear translocation using beta-galactosidase enzyme fragment complementation. Assay Drug Dev Technol 2006;4(3):263–272.

29. Gannon PO, Godin-Ethier J, Hassler M, Delvoye N, Aversa M, Poisson AO, Peant B, Alam Fahmy M, Saad F, Lapointe R, Mes-Masson AM. Androgen-regulated expression of arginase 1, arginase 2 and interleukin-8 in human prostate cancer. PLoS ONE 2011;5(8):e12107.

30. Jiang C, Lee HJ, Li GX, Guo J, Malewicz B, Zhao Y, Lee EO, Lee JH, Kim MS, Kim SH, Lu J. Potent antiandrogen and androgen receptor activities of an *Angelica gigas*-containing herbal formulation: Identification of decursin as a novel and active compound with implications for prevention and treatment of prostate cancer. Cancer Res 2006;66(1):453–463.

31. Lu S, Wang A, Dong Z. A novel synthetic compound that interrupts androgen receptor signaling in human prostate cancer cells. Mol Cancer Ther 2007;6(7):2057–2064.

32. Makkonen H, Kauhanen M, Jaaskelainen T, Palvimo JJ. Androgen receptor amplification is reflected in the transcriptional responses of vertebral-cancer of the prostate cells. Mol Cell Endocrinol 2011;331(1):57–65.

33. Sun S, Sprenger CC, Vessella RL, Haugk K, Soriano K, Mostaghel EA, Page ST, Coleman IM, Nguyen HM, Sun H, Nelson PS, Plymate SR. Castration resistance in human prostate cancer is conferred by a frequently occurring androgen receptor splice variant. J Clin Invest 2010;120(8):2715–2730.

34. Thomas PD, Campbell MJ, Kejariwal A, Mi H, Karlak B, Daverman R, Diemer K, Muruganujan A, Narechania A, PANTHER: A library of protein families and subfamilies indexed by function. Genome Res 2003;13(9):2129–2141.

35. Ma C, Quesnelle KM, Sparano A, Rao S, Park MS, Cohen MA, Wang Y, Samanta M, Kumar MS, Aziz MU, Naylor TL, Weber BL, Fakharzadeh SS, Weinstein GS, Vachani A, Feldman MD, Brose MS. Characterization CSMD1 in a large set of primary lung, head and neck, breast and skin cancer tissues. Cancer Biol Ther 2009;8(10):907–916.

36. Calvo V, Beato M. BRCA1 counteracts progesterone action by ubiquitination leading to progesterone receptor degradation and

epigenetic silencing of target promoters. Cancer Res 2011;71 (9):3422–3431.

37. Thompson ME. BRCA1 16 years later: Nuclear import and export processes. FEBS J 2010;277(15):3072–3078.

38. Shanmugam I, Cheng G, Terranova PF, Thrasher JB, Thomas CP. Li B. Serum/glucocorticoid-induced protein kinase-1 facilitates androgen receptor-dependent cell survival. Cell Death Differ 2007;14(12):2085–2094.

39. Royuela M, Ricote M, Parsons MS, Garcia-Tunon I, Paniagua R, de Miguel MP. Immunohistochemical analysis of the IL-6 family of cytokines and their receptors in benign, hyperplasic, and malignant human prostate. J Pathol 2004;202(1):41–49.

40. Godoy-Tundidor S, Cavarretta IT, Fuchs D, Fiechtl M, Steiner H, Friedbichler K, Bartsch G, Hobisch A, Culig Z. Interleukin-6 and oncostatin M stimulation of proliferation of prostate cancer 22Rv1 cells through the signaling pathways of p38 mitogen-activated protein kinase and phosphatidylinositol 3-kinase. Prostate 2005;64(2):209–216.

41. Jaaskelainen T, Makkonen H, Palvimo JJ. Steroid up-regulation of FKBP51 and its role in hormone signaling. Curr Opin Pharmacol 11 2011; (4):326–331.

42. Waltering KK, Helenius MA, Sahu B, Manni V, Linja MJ, Janne OA, Visakorpi T. Increased expression of androgen receptor sensitizes prostate cancer cells to low levels of androgens. Cancer Res 2009;69(20):8141–8149.

43. Yoshida T, Kinoshita H, Segawa T, Nakamura E, Inoue T, Shimizu Y, Kamoto T, Ogawa O. Antiandrogen bicalutamide promotes tumor growth in a novel androgen-dependent prostate cancer xenograft model derived from a bicalutamide-treated patient. Cancer Res 2005;65(21):9611–9616.

44. Bohl CE, Gao W, Miller DD, Bell CE, Dalton JT. Structural basis for antagonism and resistance of bicalutamide in prostate cancer. Proc Natl Acad Sci USA 2005;102(17):6201–6206.

45. Claessens F, Denayer S, Van Tilborgh N, Kerkhofs S, Helsen C, Haelens A. Diverse roles of androgen receptor (AR) domains in AR-mediated signaling. Nucl Recept Signal 2008;6:e008.

46. He B, Minges JT, Lee LW, Wilson EM. The FXXLF motif mediates androgen receptor-specific interactions with coregulators. J Biol Chem 2002;277(12):10226–10235.

47. Schaufele F, Carbonell X, Guerbadot M, Borngraeber S, Chapman MS, Ma AA, Miner JN, Diamond MI. The structural basis of androgen receptor activation: Intramolecular and intermolecular amino-carboxy interactions. Proc Natl Acad Sci USA 2005;102 (28):9802–9807.

48. van Royen ME, Cunha SM, Brink MC, Mattern KA, Nigg AL, Dubbink HJ, Verschure PJ, Trapman J, Houtsmuller AB. Compartmentalization of androgen receptor protein–protein interactions in living cells. J Cell Biol 2007;177(1):63–72.

49. Kaku N, Matsuda K, Tsujimura A, Kawata M. Characterization of nuclear import of the domain-specific androgen receptor in association with the importin alpha/beta and Ran-guanosine 5′-triphosphate systems. Endocrinology 2008;149(8):3960–3969.

50. Zhou F, Zhao W, Zuo Z, Sheng Y, Zhou X, Hou Y, Cheng H, Zhou R. Characterization of androgen receptor structure and nucleocytoplasmic shuttling of the rice field eel. J Biol Chem 2010;285(47):37030–37040.

51. Saporita AJ, Zhang Q, Navai N, Dincer Z, Hahn J, Cai X, Wang Z. Identification and characterization of a ligand-regulated nuclear export signal in androgen receptor. J Biol Chem 2003;278 (43):41998–42005.

52. Schutz SV, Cronauer MV, Rinnab L. Inhibition of glycogen synthase kinase-3beta promotes nuclear export of the androgen receptor through a CRM1-dependent mechanism in prostate cancer cell lines. J Cell Biochem 2010;109(6):1192–1200.

53. Cutress ML, Whitaker HC, Mills IG, Stewart M, Neal DE. Structural basis for the nuclear import of the human androgen receptor. J Cell Sci 2008;121(Pt 7):957–968.

54. Langley E, Zhou ZX, Wilson EM. Evidence for an anti-parallel orientation of the ligand-activated human androgen receptor dimer. J Biol Chem 1995;270(50):29983–29990.

55. Hodgson MC, Astapova I, Hollenberg AN, Balk SP. Activity of androgen receptor antagonist bicalutamide in prostate cancer cells is independent of NCoR and SMRT corepressors. Cancer Res 2007;67(17):8388–8395.

56. Masiello D, Cheng S, Bubley GJ, Lu ML, Balk SP. Bicalutamide functions as an androgen receptor antagonist by assembly of a transcriptionally inactive receptor. J Biol Chem 2002;277(29): 26321–26326.

57. Hodgson MC, Astapova I, Cheng S, Lee LJ, Verhoeven MC, Choi E, Balk SP, Hollenberg AN. The androgen receptor recruits nuclear receptor CoRepressor (N-CoR) in the presence of mifepristone via its N and C termini revealing a novel molecular mechanism for androgen receptor antagonists. J Biol Chem 2005; 280(8):6511–6519.

58. Ozers MS, Marks BD, Gowda K, Kupcho KR, Ervin KM, De Rosier T, Qadir N, Eliason HC, Riddle SM, Shekhani MS. The androgen receptor T877A mutant recruits LXXLL and FXXLF peptides differently than wild-type androgen receptor in a time-resolved fluorescence resonance energy transfer assay. Biochemistry 2007;46(3):683–695.

59. Masiello D, Chen SY, Xu Y, Verhoeven MC, Choi E, Hollenberg AN, Balk SP. Recruitment of beta-catenin by wild-type or mutant androgen receptors correlates with ligand-stimulated growth of prostate cancer cells. Mol Endocrinol 2004;18(10): 2388–2401.

60. Kolvenbag GJ, Furr BJ, Blackledge GR. Receptor affinity and potency of non-steroidal antiandrogens: Translation of preclinical findings into clinical activity. Prostate Cancer Prostatic Dis 1998;1(6):307–314.

61. Zhou J, Liu B, Geng G, Wu JH. Study of the impact of the T877A mutation on ligand-induced helix-12 positioning of the androgen receptor resulted in design and synthesis of novel antiandrogens. Proteins 2010;78(3):623–637.

62. Brooke GN, Parker MG, Bevan CL. Mechanisms of androgen receptor activation in advanced prostate cancer: Differential co-activator recruitment and gene expression. Oncogene 2008;27 (21):2941–2950.

63. Moehren U, Papaioannou M, Reeb CA, Grasselli A, Nanni S, Asim M, Roell D, Prade I, Farsetti A, Baniahmad A. Wild-type but not mutant androgen receptor inhibits expression of the hTERT telomerase subunit: A novel role of AR mutation for prostate cancer development. FASEB J 2008;22(4):1258–1267.

64. Lee EC, Zhan P, Schallhom R, Packman K, Tenniswood M. Antiandrogen-induced cell death in LNCaP human prostate cancer cells. Cell Death Differ 2003;10(7):761–771.

65. Sahu B, Laakso M, Pihlajamaa P, Ovaska K, Sinielnikov I, Hautaniemi S, Janne OA. FoxA1 specifies unique androgen and glucocorticoid receptor binding events in prostate cancer cells. Cancer Res 2012;73:1570–1580.

SUPPORTING INFORMATION

Additional supporting information may be found in the online version of this article at publisher's website.

Figure S1. Enzalutamide inhibits agonist induced transcription of the AR-dependent gene TMPRSS2. TMPRSS2 mRNA levels in wild type LNCaP (LNCaP-wt) **(A, B)** were measured by qRT-PCR. Cells were treated for 8 h with DMSO (vehicle), enzalutamide alone or bicalutamide alone **(A)** or enzalutamide or bicalutamide in the presence of 1 nM of DHT **(B)**. Data were normalized to expression levels of α-tubulin and the value of TMPRSS2 expression in vehicle-treated cells was set to 1.0. Data are displayed as mean $\pm$ SEM (error bars), n = 6. (***p < 0.001, **p < 0.01, *p < 0.05, each treatment was tested individually against vehicle using ANOVA with Bonferroni post test).

Figure S2. Representative images of in HEK-293 live cells expressing AR-YFP showing the cellular fluorescence distribution in response to DHT 1 nM vs. drug treatments (in rows), from top to bottom: vehicle treated cells (A); bicalutamide 1 μM (B); bicalutamide 10 μM (C); enzalutamide 1 μM (D) and 10 μM (E) at 1 hour intervals. Cells were pre-treated with enzalutamide (1 or 10 μM) or bicalutamide (1 or 10 μM) for 2 hours and then co-treated with 1 nM DHT for three hours in the presence of enzalutamide or bicalutamide. Imaging began immediately before DHT addition (t ′ = 0). Scale bar represents 10 μm.

Figure S3. Dose-response of 6-α-[F]-testosterone (6AFT) (■); bicalutamide (Δ); and enzalutamide (●), induced AR nuclear translocation. The fraction of AR receptor that translocates to the nucleus in the presence of 6AFT was measured using PathHunter NHRPro HEK-wtAR cell lines.

Figure S4. (A) Components Analysis (PCA) plot was performed using covariance for the dispersion matrix and normalized scaling. This analysis was done to illustrate the level of spread between the samples and experimental groups: vehicle (a); DHT 100 nM (b); enzalutamide 1 μM (c); enzalutamide 10 μM (d); DHT 100 nM + enzalutamide 1 μM (e); DHT 100 nM + enzalutamide 10 μM (f). (B) Hierarchical clustering was carried out using correlation distance as the distance metric and average linkage between clusters to perform the clustering. This analysis is a non-supervised method that is done to illustrate potential relationships between the mRNA expression profiles of the different samples, after filtering data sets for ANOVA significance (p<0.05) between treatments and vehicle treated cells (A, vehicle; B, DHT 100 nM; C, enzalutamide 1 μM; D, enzalutamide 10 μM; E, DHT 100 nM + enzalutamide 1 μM; F, DHT 100 nM + enzalutamide 10 μM). Three replicates were conducted for each condition.

Table SI. Summary of genes with at least two fold changes derived from microarray expression analysis in LNCaP cells treated with DHT and enzalutamide